(Received 28 February 2024, Accepted 19 May 2024, Scheduled 28 May 2024)

Design of a CSRR Dual-Port Patch Antenna with Elliptical Slots on Ground Plane for Wireless Communication

Manjula Sanugomula and Ketavath Kumar Naik*

Antenna Research Laboratory, Department of Electronics and Communication Engineering
Koneru Lakshmaiah Education Foundation (KLEF) Deemed to be University, Vaddeswaram, Guntur-522502, India

ABSTRACT: This paper introduces a complementary split ring resonator (CSRR) patch antenna with elliptical slots on the ground plane for wireless communication, significantly amplified by placing two conducting elements over the substrate. The dimensions of the designed CSRR dual element multiple-input-multiple-output (MIMO) antenna are $16 \times 32\,\text{mm}^2$ ($0.66\lambda \times 1.33\lambda$). In this paper, the CSRR dual element MIMO antenna with an elliptical DGS resonates at 11.523 GHz, 12.305 GHz, and 15.178 GHz with reflection coefficients of -22.67 dB, -26.25 dB, and -47.65 dB, respectively. It presents an impressive wide impedance bandwidth of 1.462 GHz covering 11.523 GHz and 12.305 GHz resonating frequencies and 1.446 GHz at 15.178 GHz resonance. The proposed design gives a gain of 5.29 dBi, 6.12 dBi, and 5.97 dBi for the resonating frequencies, respectively. The results show a minimum envelope correlation coefficient (< 0.025) and a significant diversity gain (> 9.85) across the entire bandwidth. The measured results are close to the simulated ones, confirming the efficiency of the triple resonating frequencies with wideband, high-gain antenna design used for wireless communications for faster data transmission rates.

1. INTRODUCTION

In current wireless communication systems, an antenna plays a crucial role, requiring compact and intelligent designs, particularly for high data rates. Microstrip patch antennas present advantages including low profile, compact dimensions, and effortless integration into high-frequency systems [1]. In the real time of wireless communications, emphasizing size and installation convenience stands as a key consideration of an antenna [2]. Microstrip antennas are the best option for satisfying the increasing demand for low profile antennas. The antennas used in wireless communication need to provide high reflection coefficient, wide bandwidth, and high gain as key parameters. But patch antennas characteristically exhibit a limited impedance bandwidth and comparatively lower gain [3]. To overcome these challenges, many approaches have been proposed, including substrate thickening, integrating slots on the patch [4], and creating defected ground structures (DGSs) [5].

Typically, implementing structures and geometries of patches [6] or slots in antennas and repetition of a structure like fractals [7] tends to reduce their physical dimensions and generate multiband responses in their resonating properties [8]. The iterations involved in generating fractal configurations enable the creation of extended directions and increased surface areas within limited volumes [9]. Placing an elliptical slot over the ground emerges as a highly effective solution to amplify performance, widen the impedance bandwidth, and have high gain [10]. The focus on wideband technology has risen significantly in wireless communication, forced by its ability to provide high data rates at low cost [11]. Reflection and diffraction, inherent phenomena in dense mediums, introduce multipath fading in conventional wideband technology. The introduction of MIMO technology attempts to avoid the challenges posed by multipath fading while simultaneously improving the transmission quality within communication systems [12].

In modern portable wireless systems, the limited space presents a challenge for MIMO antennas [13]. Typically, these antennas require a minimum of two radiating elements positioned at specific distances to ensure isolation [14]. Introducing slits and slots on the radiators [15] and ground [16] helps in reducing the mutual interference between adjacent antennas [17]. Circular monopole antenna gives low voltage standing wave ratio (VSWR) over ultra-wideband (UWB) [18], and multiband [19] and is used in UWB communications. Introducing the concept of iterations [20] to a circular patch antenna gives good gain with appreciable bandwidth [21]. At least two elements are required as a MIMO antenna gets wider bandwidth [22] and provides multiple resonating frequencies [23]. Wireless applications like GPS, WiMAX, WLAN, and Satellite require multiple bands with compact antenna [24]. In [25], a miniaturized single feed multiband antenna is presented. Compact monopole antenna generates multibands [26].

This paper presents a CSRR patch antenna with elliptical slots on the ground plane, specifically designed for efficient performance in wireless communication for high data rate transmission at different resonating frequencies 11.523 GHz, 12.305 GHz, and 15.178 GHz. The designed antenna is simulated using CST Microwave studio to get optimum results [27]. The design integrates a central circular slot on the radiating el-

* Corresponding author: Ketavath Kumar Naik (drkumarkn@hotmail.com).

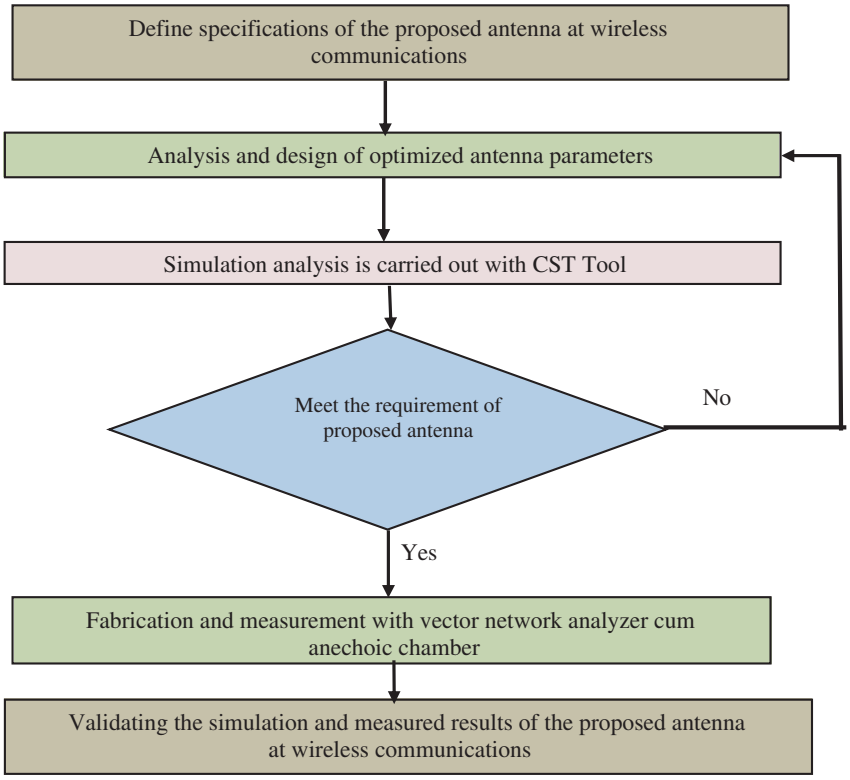

FIGURE 1. Flow Chart of an Antenna Design.

ement, measuring 0.5 mm in width, accompanied by another elliptical slot positioned with a 2 mm distance along the x-axis and a 1.5 mm distance along the y-axis from the center slot of the patch. Over ground material, two slots were etched with multiple iterations of ellipse to achieve multiple resonating frequencies for wireless communication. Introducing a CSRR to the patch has an impact on various antenna performance aspects, including reflection coefficient, gain, bandwidth, and resonance shifts.

The antenna proposed in this paper presents reflection coefficients (S_{11}) of -22.67 dB, -26.25 dB, and -47.65 dB at resonating frequencies 11.523 GHz, 12.305 GHz, 15.178 GHz, respectively. CSRR facilitated enhancing gain characteristics, and multiple iterations of elliptical slots over the ground are responsible for getting multiple resonating frequencies. While the dual element concept as MIMO effectively reduced multipath fading, it led to reduced interference. The gain values at the resonating frequencies are 5.29 dBi, 6.12 dBi, and 5.97 dBi, respectively. The remarkable coherence between the simulated and measured outcomes validates the designed antenna that works as the prime choice for satellite communication. It results in low envelope correlation coefficient (ECC), high diversity gain (DG), and notably minimal mutual coupling among the radiating elements. A flowchart to design an antenna is presented in Fig. 1.

2. ANTENNA DESIGN

The basic structure of a microstrip patch antenna includes a substrate plane, a ground plane, a microstrip feed, and a patch, which can take on various shapes such as ellipse, circle, rectangle, and beyond. We designed a microstrip patch antenna with a circular shape on an FR4 substrate for enhanced performance and efficiency. After the rectangular patch antenna, circular patch antenna emerges as another widely chosen geometry among microstrip antennas, considered for its relatively compact dimensions. In this proposed design, 't_s' represents the substrate's thickness, while 'R' denotes the radius of the circular patch. The resonating frequency of the proposed patch antenna is determined from a radius of the patch using the following expression (1) [10].

$$f_r = \frac{8.794}{r_e\sqrt{\varepsilon_r}} \tag{1}$$

where f_r is the resonant frequency of the patch, ε_r the relative permittivity of the substrate, and r_e the effective radius of the circular patch given by (2) [10].

$$r_e = R\left[1+\frac{2t_s}{\pi R\varepsilon_r}\left\{\ln\left(\frac{R}{2t_s}\right)+(1.41\varepsilon_r+1.77)+\frac{t_s}{R}(0.268\varepsilon_r+1.65)\right\}\right]^{\frac{1}{2}} \tag{2}$$

where R is the radius of the circular patch and t_s the height of the substrate.

Figure 2 illustrates the evaluation steps of the proposed CSRR dual element antenna. Fig. 2(a) displays the antenna's

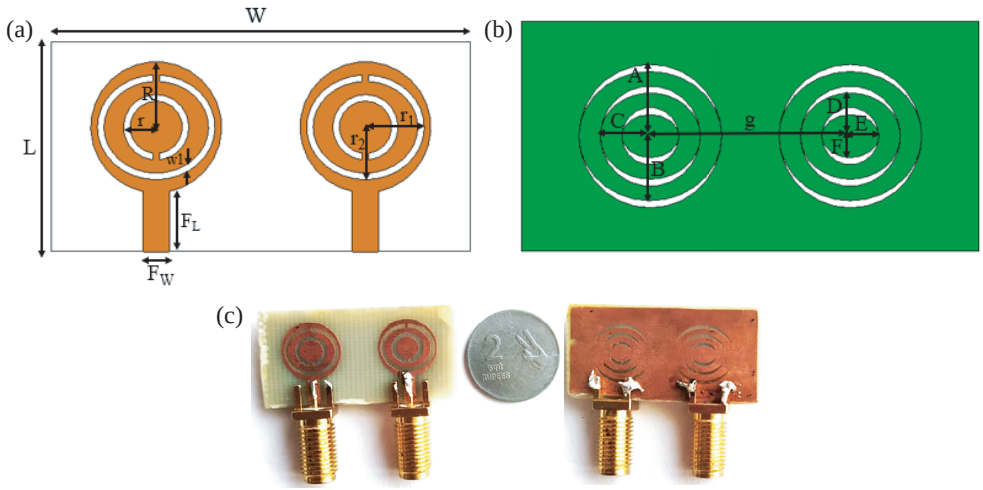

FIGURE 2. (a) Top View of the Proposed MIMO Antenna. (b) Bottom View-Ground with fractal DGS. (c) Fabricated Prototype.

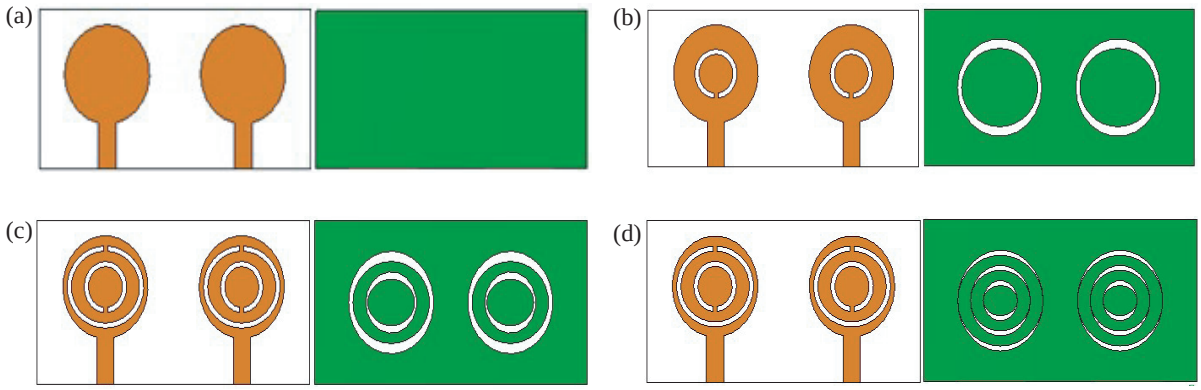

FIGURE 3. Evaluation of antenna Design. (a) Ant. 1. (b) Ant. 2. (c) Ant. 3. (d) Ant. 4.

top view, while Fig. 2(b) provides the bottom view for a comprehensive understanding of its configuration with parameters. Fig. 2(c) presents the prototype of the proposed antenna. The antenna is designed on a substrate of FR-4 having a dielectric constant ε_r of 4.3, loss tangent of 0.025, and thickness measuring 1.6 mm. Multiple iterations of elliptical slots were created over ground. This approach increases the generation of multiple frequency bands, but the antenna performance of multiple resonating frequencies decreases. CSRR slots were created over the patch to improve the antenna parameters at multiple resonating frequencies. Dimensions of the optimized parameters for the proposed antenna are presented in Table 1.

TABLE 1. Dimensions of the optimized parameters for the proposed antenna.

Parameter	Value (mm)	Parameter	Value (mm)
L	16	r_2	4
W	32	g	9
F_L	4.5	A	5
F_W	2	B	4.5
R	5	C	3
r	2.5	D	2.5
r_1	4.5	E	1
w_1	0.5	F	0.5

2.1. Evaluation of the Two-Port MIMO Antenna Design

Figure 3 illustrates the sequential design stages for the dual elements integrated into the proposed antenna. Initially, Ant. 1 (Fig. 3(a)) was developed with a basic circular-shape radiator using copper and a full ground plane using perfectly electrically conducting (PEC) material (Iteration-0). It is simulated using CST Studio to observe specific outcomes for the design. In this, single resonating frequency is obtained, and antenna parameters are not good enough. To enhance the antenna parameters further, open circular slot was etched with a radius of 2.5 mm and width of 0.5 mm over the patch, and in parallel two elliptical shaped slots were created consisting of a 5 mm slot width over the ground (Iteration-1) in Ant. 2 as shown in Fig. 3(b). This modification resulted in reducing the bandwidth and increased gain. To achieve multiple resonating frequencies, additional slots were etched over the patch and ground in Ant. 3 as shown in Fig. 3(c). To get additional bands without compromising the antenna parameters, in Ant. 4 one more slot was

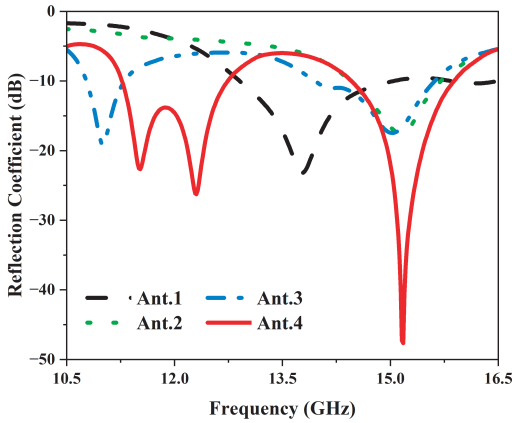

FIGURE 4. Reflection coefficient values at different stages of antenna configuration.

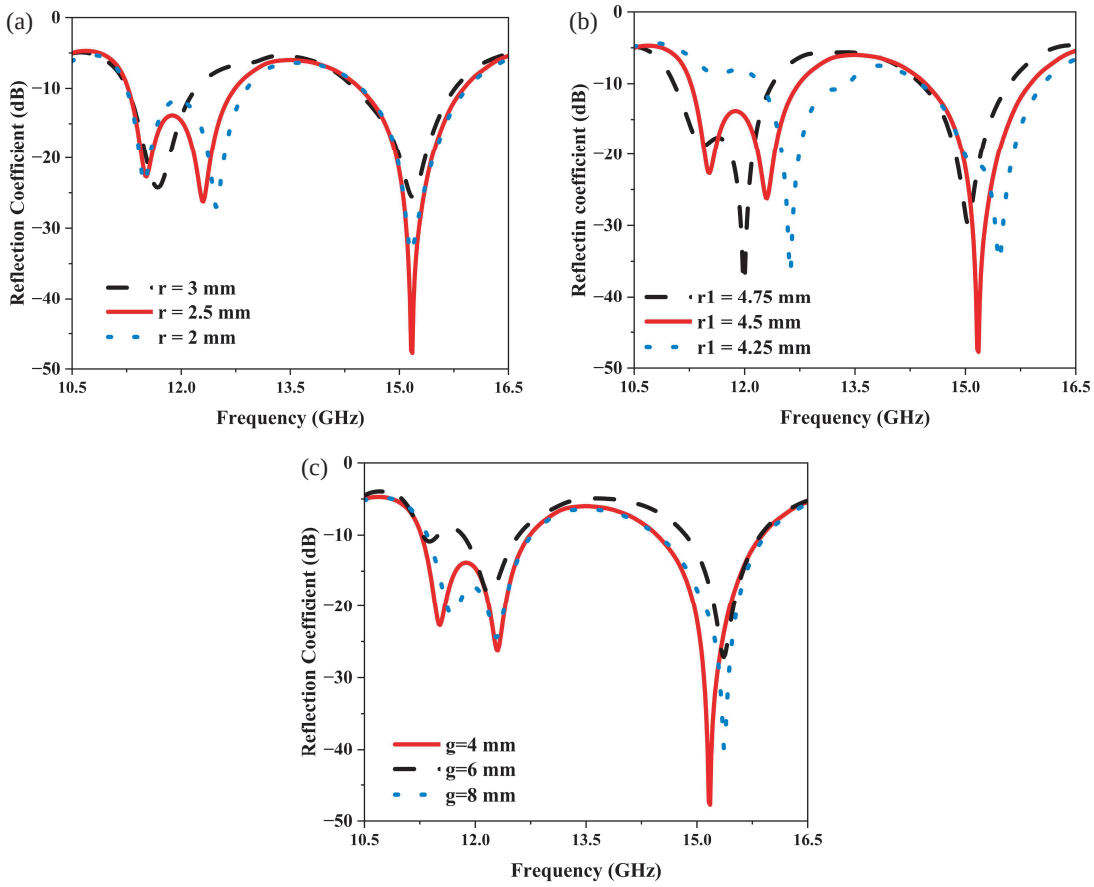

FIGURE 5. Reflection coefficient for different values of (a) Circular slot radius (r), (b) Elliptical slot radius (r_1), (c) Separation between slots over ground (g).

etched over the ground (Iteration-3), and the dimensions of the elliptical slot were also adjusted in parallel to increase the current path as shown in Fig. 3(d).

Figure 4 shows the simulated reflection coefficient values for different evaluation steps of antenna configuration, and Table 2 tabulates the antenna parameter values for different stages of evaluation. In the results, the proposed design resonates at 11.523 GHz, 12.305 GHz, and 15.178 GHz with reflection coefficients -22.67 dB, -26.25 dB, and -47.65 dB, and wide impedance bandwidths as 1.468 GHz, 1.443 GHz respectively as shown in Fig. 4.

2.2. Parametric Analysis

Fig. 5 shows the parametric analysis of the proposed antenna's behavior, specifically investigating the impacts of lot dimen-

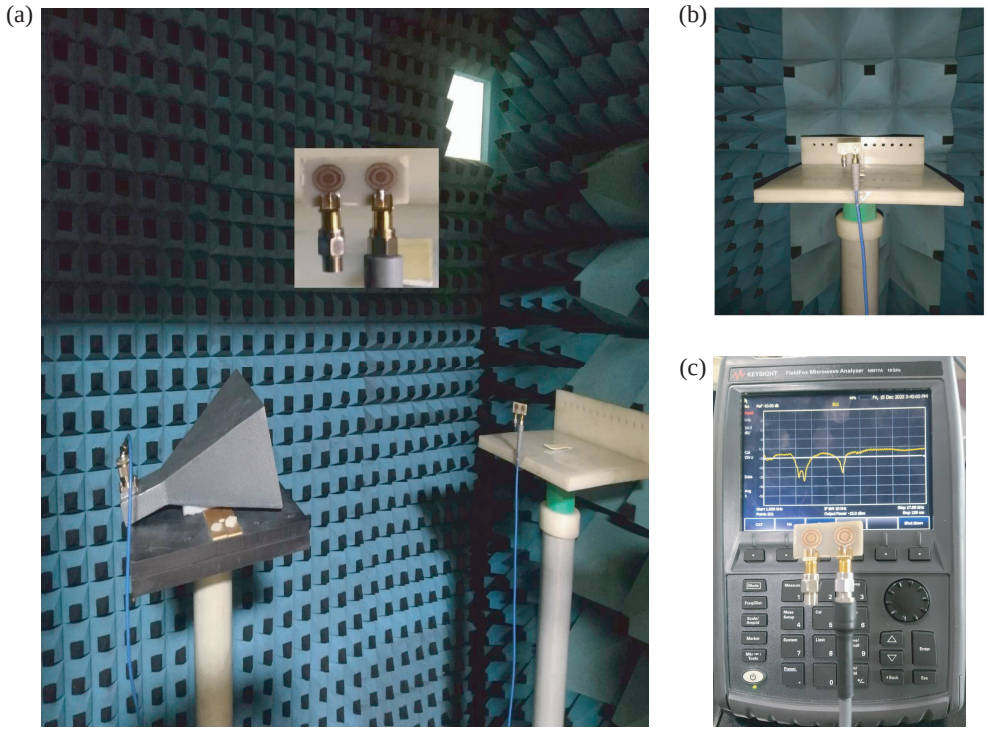

FIGURE 6. (a) The measurement setup in anechoic chamber, (b) close view of the anechoic chamber, (c) Reflection coefficient in vector network analyzer.

TABLE 2. Antenna parameters at different stages of antenna design.

Design	Operating Frequency (GHz)	Reflection Coefficient (dB)	Bandwidth (GHz)	Gain (dBi)
Ant. 1	13.784	−23.18	2.03	5.68
Ant. 2	15.161	−17.56	1.24	6.34
Ant. 3	11.013	−19.123	0.526	5.51
	15.025	−17.466	1.65	5.47
Ant. 4	15.178	−47.65	1.433	5.97
	12.305	−26.25	1.468	6.12
	11.523	−22.67	1.468	5.29

sions (r, r_1), and the distance between the etched slots over ground (g) is thoroughly examined using CST software [27].

2.2.1. Effect of Circular Slot Radius (r)

In Fig. 5(a), a parametric analysis explores various radius values. As the r value moves from resonating frequency to higher or lower one, the reflection coefficient values are affected. The reflection coefficient values for $r = 3$ mm are -24.24 dB, -25.59 dB at 11.676 GHz, 15.178 GHz, respectively, for $r = 2.5$ mm are -22.688 dB, -26.23 dB, -47.73 dB at 11.523 GHz, 12.305 GHz, 15.178 GHz, respectively, and for $r = 2$ mm are -23.85 dB, -26.977 dB, -33.6 dB at 11.489 GHz, 12.475 GHz, 15.161 GHz, respectively. The frequency shifts owing to the distractions in the current path. Balancing bandwidth and reflection coefficients, $r = 2.5$ mm was identified as the optimized value.

2.2.2. Effect of Elliptical Slot Radius (r_1)

In Fig. 5(b), a parametric analysis explores various radius values. As the r_1 value moves from resonating frequency to higher or lower one, the reflection coefficient values are affected. The reflection coefficient values for $r_1 = 4.75$ mm are -38.25 dB, -29.77 dB at 11.99 GHz, 15.042 GHz, respectively, for $r_1 = 4.5$ mm are -22.688 dB, -26.23 dB, -47.73 dB at 11.523 GHz, 12.305 GHz, 15.178 GHz, respectively, and for $r_1 = 4.25$ mm are -36.67 dB, -35 dB, at 12.611 GHz, 15.467 GHz, respectively. The frequency shifts owing to the distractions in the current path. $r_1 = 4.5$ mm was

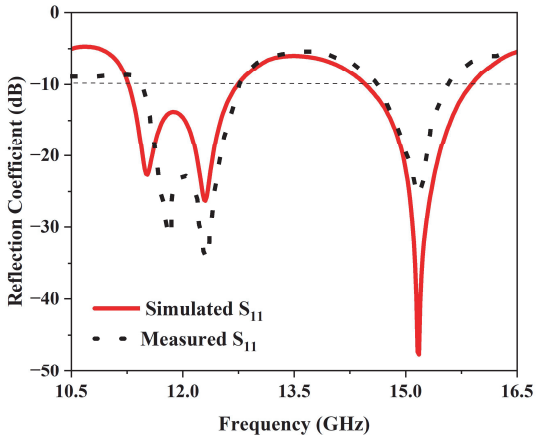

FIGURE 7. Simulated and Measured Reflection Coefficient.

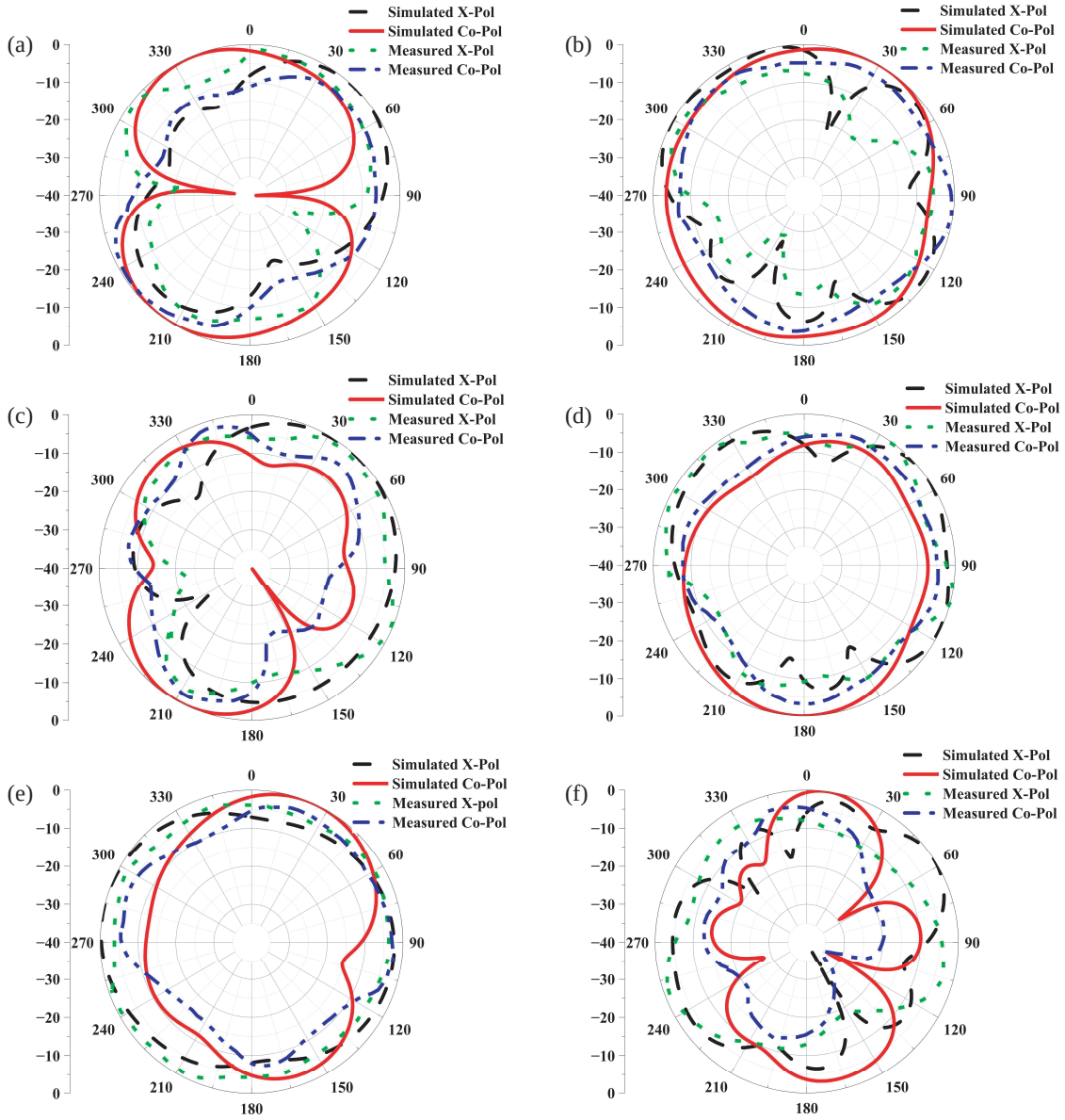

FIGURE 8. Simulated and Measured x-pol, Co-pol of (a) *E*-Plane at 11.523 GHz, (b) *H*-Plane at 11.523 GHz, (c) *E*-Plane at 12.305 GHz, (d) *H*-Plane at 12.305 GHz, (e) *E*-Plane at 15.178 GHz, (f) *H*-Plane at 15.178 GHz.

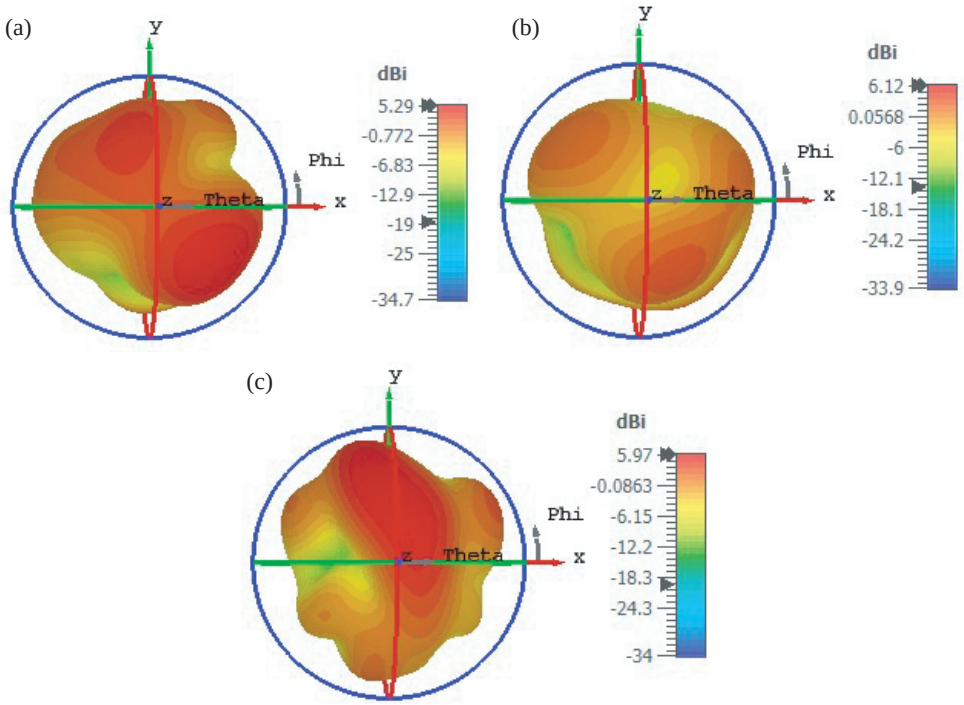

FIGURE 9. 3D gain plot (a) at 11.523 GHz, (b) at 12.305 GHz, (c) at 15.178 GHz.

identified as the optimized value for getting triple bands and wider bandwidths compared to 4.75 mm and 4.25 mm. For $r_1 = 4.75$ mm, the slot is very close to the patch edge, so, the current distribution path deviated results in poor parameter values compared to $r_1 = 4.5$ mm.

3. EFFECT OF GROUND SEPARATION (g)

In the design of the proposed antenna, the ground includes two slots as DGS, crucial for achieving key antenna parameters. The positioning of these etched slots significantly impacts antenna performance. Therefore, an analysis was conducted to study the impact of separation between the two slots using CST. In Fig. 5(c), the reflection coefficient values are represented across various values from edge to edge of the slots. The simulated results revealed that as the separation between the slots increased, the parameter values declined because slots etched in the ground plane under the microstrip line changed the effective capacitance and inductance of microstrip line by adding slot resistance, capacitance, and inductance. 4 mm was observed as the optimized value for the edge-to-edge gap between slots (g).

4. RESULTS AND DISCUSSIONS

The measurement setup in an anechoic chamber and vector network analyzer (VNA) results are also presented in Figs. 6(a), (b), (c) for validating the results.

4.1. *S*-Parameter Results

Figure 7 shows a comparison result between the reflection coefficients (S_{11}) of the simulated and measured results. CST Microwave Studio shows wide bandwidths from 11.269 GHz to 12.737 GHz (1.468 GHz) and from 14.457 GHz to 15.9 GHz (1.443 GHz). The resonating frequencies in the wide impedance bandwidth range are 11.523 GHz, 12.305 GHz, and 15.178 GHz with reflection coefficients -22.67 dB, -26.25 dB, and -47.65 dB, respectively. A good agreement between simulated and measured results has been observed.

4.2. Radiation Pattern

The simulated and measured results of radiation patterns are compared in Fig. 8 at resonating frequencies 11.523 GHz, 12.305 GHz, and 15.178 GHz. A good agreement in the comparison of the simulated and measured results has been observed. Fig. 9 shows the obtained 3D gain plot (a) at 11.523 GHz as 5.29 dBi, (b) at 12.305 GHz as 6.12 dBi, and (c) at 15.178 GHz as 5.97 dBi.

4.3. Surface Current Distributions

Surface current in antennas signifies the flow of electric current along the surface of an antenna element, particularly when the dimensions closely match the wavelength of the electromagnetic wave they transmit or receive. Fig. 10 represents the surface current distributions at the operating frequencies when both ports are excited independently. The current density at the resonant frequency shows a greater amount of accumulated current on the radiating patch.

4.4. Envelope Correlation Coefficient and Diversity Gain

For optimal pattern diversity in utilizing antenna elements, a fundamental requirement is for their radiation patterns to exhibit minimal correlation. When multiple element antenna ap-

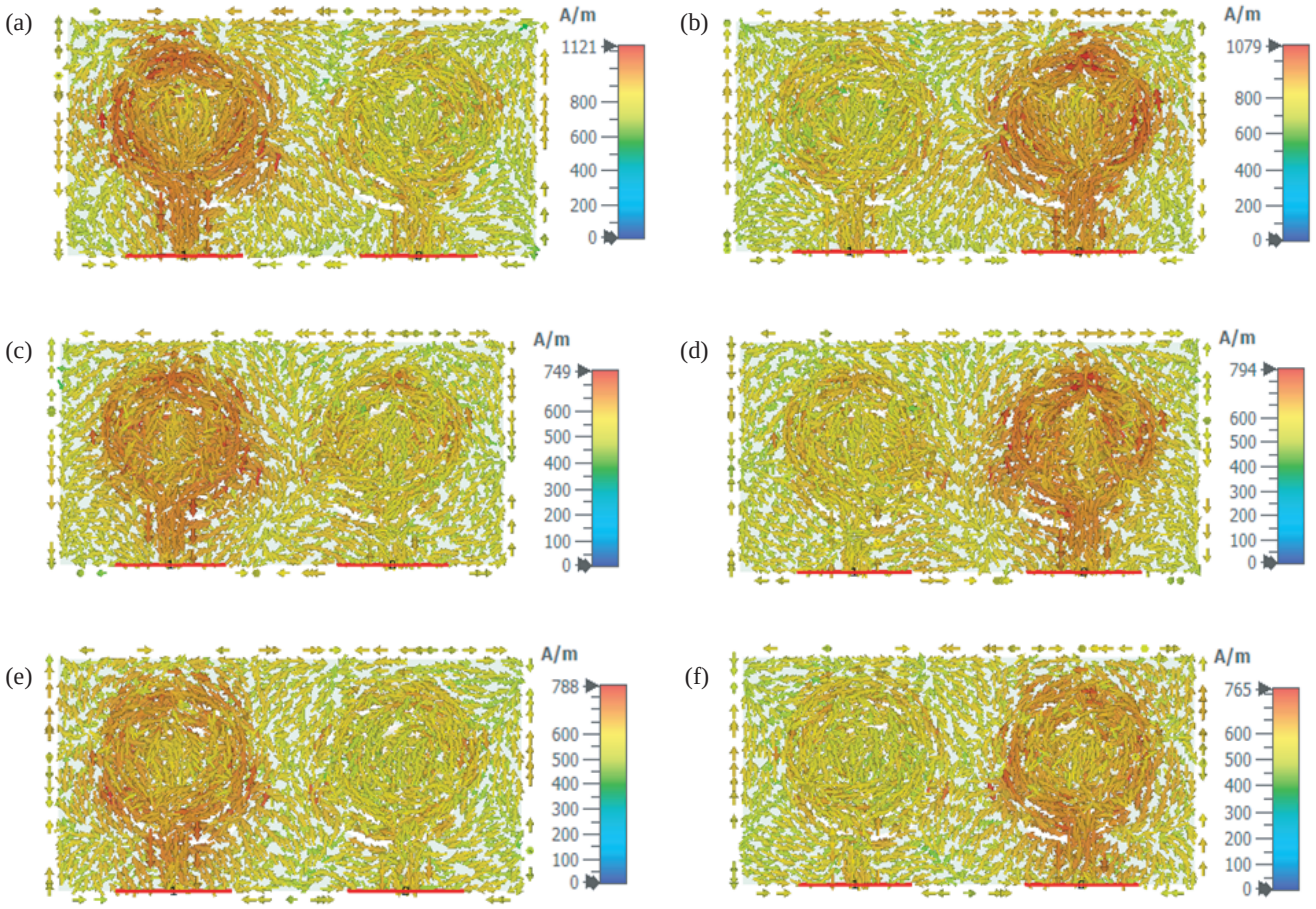

FIGURE 10. Surface Currents at (a) Port-1 excited at 11.523 GHz, (b) Port-2 excited at 11.523 GHz, (c) Port-1 excited at 12.305 GHz, (d) Port-2 excited at 12.305 GHz, (e) Port-1 excited at 15.178 GHz, (f) Port-2 excited at 15.178 GHz.

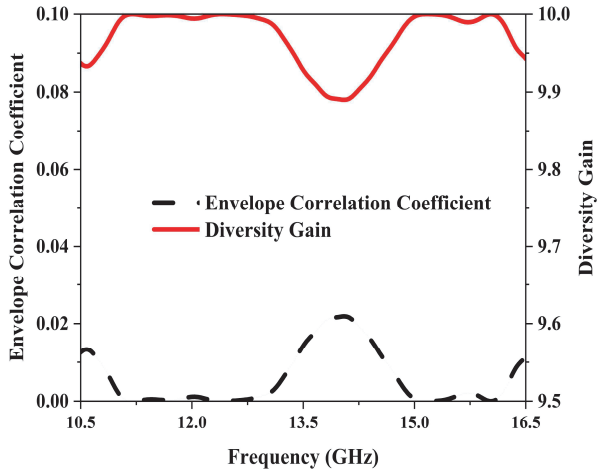

FIGURE 11. ECC and Diversity Gain Plot of the proposed antenna.

plications are considered, the envelope correlation coefficient (ECC) can be computed using either the far-field radiation pattern or scattering parameter.

Calculating the ECC parameter from 3D far-field radiation pattern measurements is ideal, but it can become difficult. Therefore, ECC calculations based on S-parameters are preferred and prioritized. The ECC and DG between element i ($i = 1$) and element j ($j = 2$) can be computed from scattering parameters using the following Equations (3), (4) [12].

$$ECC_{ij} = \frac{|S_{ii}^* S_{ij} + S_{ji}^* S_{jj}|^2}{[1 - (|S_{ii}|^2 + |S_{ji}|^2)][1 - (|S_{jj}|^2 + |S_{ij}|^2)]} \quad (3)$$

TABLE 3. Comparative study of the proposed antenna to the existing antennas.

Ref. No	Substrate	Dimensions in wavelength	Resonating Frequency (GHz)	Bandwidth (GHz)	Gain (dBi)	Applications
[2]	FR-4	$0.57\lambda\times$ 0.71λ	6.6 9.4	0.41 0.4	4.77 6.29	Satellite Communication and Radar Applications
[3]	FR-4	$0.5\lambda\times$ 0.31λ	1.91 2.21	0.62	9.37	Wireless Systems
[6]	RT Duriod	$2.41\lambda\times$ 1.88λ	4.19 8.79 13	0.43 0.4 1	5.01 5.42 7.46	Radio Communication, Satellite Communications
[10]	FR-4	$1.9\lambda\times$ 2.28λ	13.67 15.28	0.85 1.14	8.01 6.01	KU Band Applications
[12]	Polyimide	$1.33\lambda\times$ 1.33λ	12.9 16.5	0.3 0.35	9.62 9.98	Wireless Applications
[23]	FR-4	$1.06\lambda\times$ 1.06λ	2.4 2.9 5.8	0.2 0.19 0.19	3.94 3.80 4.32	WLAN Applications
[24]	F4B	$0.37\lambda\times$ 0.26λ	1.6 3.5 5.5	0.42 0.59 1.5	1.81 3.52 4.36	GPS/WiMAX/ WLAN Applications
[26]	FR-4	$0.4\lambda\times$ 0.35λ	2.4 5.2 5.8	0.12 1.40 1.56	NA	WiMAX/WLAN Applications
Proposed Antenna	FR-4	$0.66\lambda\times$ 1.33λ	11.523 12.305 15.178	1.468 (11.27–12.738) 1.433 (14.46–15.9)	5.29 6.12 5.97	Wireless Communications

NA: Not available

$$\text{Diversity Gain (DG)} = 10\sqrt{1 - |ECC_{ij}|^2} \tag{4}$$

The S-parameter approach yields ECC values below 0.025 and DG values exceeding 9.85. Normalized ECC and DG graphical representation is presented in Fig. 11. In Table 3, the comparisons of existing antennas to the proposed antenna are summarized. It is observed that the bandwidth is more, and the size of the proposed antenna is also less.

5. CONCLUSION

This paper presents a design of a CSRR patch antenna with elliptical slots on ground plane for wireless communication. Employing CSRR and multiple slots over the ground as DGS enables triple bands, wideband capability, and high gain, which are essential for effective wireless communication. The recommended antenna is compact, measuring $16 \times 32\,\text{mm}^2$ ($0.66\lambda \times 1.33\lambda$). The presented antenna resonates precisely at 11.523 GHz, 12.305 GHz, and 15.178 GHz with reflection coefficients of -22.67 dB, -26.25 dB, and -47.65 dB, respectively. It presents an impressive wide impedance bandwidth of 1.468 GHz covering 11.523 GHz and 12.305 GHz resonating frequencies and 1.433 GHz bandwidth at 15.178 GHz resonating frequency. The gains were observed at resonating frequencies as 5.29 dBi, 6.12 dBi, and 5.97 dBi, respectively. Far-field characteristics of the E-plane and H-plane were also observed at resonating frequencies. To validate the diversity performance, simulated results demonstrate ECC (below 0.025) and DG (above 9.85). The resultant resonating frequencies are suitable for downlink satellite communication, uplink satellite communication, and mobile applications, respectively.

ACKNOWLEDGEMENT

This work was supported by the SERB, Department of Science and Technology (DST), New Delhi, India. (Grant No. 1: SB/FTP/ETA-0179/2014, Grant No. 2: EEQ/2016/000754.)

REFERENCES

[1] Garg, R., P. Bhartia, I. Bahl, and I. B. A. Ittiboon, *Microstrip Antenna Design Handbook*, Artech House, 2001.

[2] Kumar Naik, K. and P. A. V. Sri, "Design of concentric circular ring patch with DGS for dual-band at satellite communication and radar applications," *Wireless Personal Communications*, Vol. 98, 2993–3001, 2018.

[3] Islam, M. T., M. N. Shakib, and N. Misran, "Broadband E-H shaped microstrip patch antenna for wireless systems," *Progress In Electromagnetics Research*, Vol. 98, 163–173, 2009.

[4] Dastranj, A., A. Imani, and M. Naser-Moghaddasi, "Printed wide-slot antenna for wideband applications," *IEEE Transactions on Antennas and Propagation*, Vol. 56, No. 10, 3097–3102, 2008.

[5] Weng, L. H., Y.-C. Guo, X.-W. Shi, and X.-Q. Chen, "An overview on defected ground structure," *Progress In Electromagnetics Research B*, Vol. 7, 173–189, 2008.

[6] Naik, K. K., G. Dattatreya, R. P. S. Chaitanya, R. Palla, and S. S. Rani, "Enhancement of gain with corrugated Y-shaped patch antenna for triple-band applications," *International Journal of RF and Microwave Computer-Aided Engineering*, Vol. 29, No. 3, e21624, 2019.

[7] Weng, W.-C. and C.-L. Hung, "An H-fractal antenna for multiband applications," *IEEE Antennas and Wireless Propagation Letters*, Vol. 13, 1705–1708, 2014.

[8] Werner, D. H. and S. Ganguly, "An overview of fractal antenna engineering research," *IEEE Antennas and Propagation Magazine*, Vol. 45, No. 1, 38–57, 2003.

[9] Darimireddy, N. K., R. R. Reddy, and A. M. Prasad, "A miniaturized hexagonal-triangular fractal antenna for wide-band applications," *IEEE Antennas and Propagation Magazine*, Vol. 60, No. 2, 104–110, 2018.

[10] Naik, K. K. and P. A. V. Sri, "Design of hexadecagon circular patch antenna with DGS at Ku band for satellite communications," *Progress In Electromagnetics Research M*, Vol. 63, 163–173, 2018.

[11] Azari, A., "A new super wideband fractal microstrip antenna," *IEEE Transactions on Antennas and Propagation*, Vol. 59, No. 5, 1724–1727, 2011.

[12] Phaneendra, C. N. and K. K. Naik, "Design of dual band MIMO antenna with rhombus shape for wireless applications," *Progress In Electromagnetics Research M*, Vol. 124, 63–70, 2024.

[13] Liu, L., S. W. Cheung, and T. I. Yuk, "Compact MIMO antenna for portable devices in UWB applications," *IEEE Transactions on Antennas and Propagation*, Vol. 61, No. 8, 4257–4264, 2013.

[14] Addepalli, T. and V. R. Anitha, "Design and parametric analysis of hexagonal shaped MIMO patch antenna for S-band, WLAN, UWB and X-band applications," *Progress In Electromagnetics Research C*, Vol. 97, 227–240, 2019.

[15] Lee, K.-F., S. L. S. Yang, and A. A. Kishk, "Dual-and multiband U-slot patch antennas," *IEEE Antennas and Wireless Propagation Letters*, Vol. 7, 645–647, 2008.

[16] Elftouh, H., N. A. Touhami, M. Aghoutane, S. E. Amrani, A. Tazón, and M. Boussouis, "Miniaturized microstrip patch antenna with defected ground structure," *Progress In Electromagnetics Research C*, Vol. 55, 25–33, 2014.

[17] Sharma, N. and S. S. Bhatia, "Ultra-wideband fractal antenna using rhombus shaped patch with stub loaded defected ground plane: Design and measurement," *AEU — International Journal of Electronics and Communications*, Vol. 131, 153604, 2021.

[18] Khan, S., J. Hu, J. Xiong, and S. He, "Circular fractal monopole antenna for low VSWR UWB applications," *Progress In Electromagnetics Research Letters*, Vol. 1, 19–25, 2008.

[19] Abutarboush, H. F., H. Nasif, R. Nilavalan, and S. W. Cheung, "Multiband and wideband monopole antenna for GSM900 and other wireless applications," *IEEE Antennas and Wireless Propagation Letters*, Vol. 11, 539–542, 2012.

[20] Levy, M., S. Bose, A. V. Dinh, and D. S. Kumar, "A novelistic fractal antenna for ultra wideband (UWB) applications," *Progress In Electromagnetics Research B*, Vol. 45, 369–393, 2012.

[21] Hwang, K. C., "A modified sierpinski fractal antenna for multiband application," *IEEE Antennas and Wireless Propagation Letters*, Vol. 6, 357–360, 2007.

[22] Naik, K. K., "Improvement of wider bandwidth using dual E–shaped antenna for wireless communications in 5G applications," *Analog Integrated Circuits and Signal Processing*, Vol. 109, No. 1, 93–101, 2021.

[23] Aminu-Baba, M., M. K. A. Rahim, F. Zubir, A. Y. Iliyasu, K. I. Jahun, M. F. M. Yusoff, M. M. Gajibo, A. A. Pramudita, and I. K. C. Lin, "A compact triband miniaturized MIMO antenna for WLAN applications," *AEU — International Journal of Electronics and Communications*, Vol. 136, 153767, 2021.

[24] Chen, S., M. Fang, D. Dong, M. Han, and G. Liu, "Compact multiband antenna for GPS/WiMAX/WLAN applications," *Microwave and Optical Technology Letters*, Vol. 57, No. 8, 1769–1773, 2015.

[25] Boukarkar, A., X. Q. Lin, Y. Jiang, and Y. Q. Yu, "Miniaturized single-feed multiband patch antennas," *IEEE Transactions on Antennas and Propagation*, Vol. 65, No. 2, 850–854, 2017.

[26] Zaman, W., H. Ahmad, and H. Mehmood, "A miniaturized meandered printed monopole antenna for triband applications," *Microwave and Optical Technology Letters*, Vol. 60, No. 5, 1265–1271, 2018.

[27] https://www.3ds.com/products/simulia/cst-studio-suite.